

Spectral characterization of a photonic bandgap fiber for sensing applications

S. Hashem Aref,^{1,2,3,*} Rodrigo Amezcua-Correac,⁴ Joel P. Carvalho,^{1,5}
Orlando Frazão,¹ José L. Santos,^{1,5} Francisco M. Araújo,¹
Hamid Latifi,³ Faramarz Farahi,⁶ Luis A. Ferreira,¹
and Jonathan C. Knight⁴

¹Instituto de Engenharia de Sistemas e Computadores do Porto,
Rua do Campo Alegre 687, 4169-007 Porto, Portugal

²Department of Physics, University of Qom, 37165 Qom, Iran

³Laser and Plasma Research Institute, Shahid Beheshti University, Evin, Tehran, Iran

⁴Department of Physics, University of Bath, Claverton Down, Bath BA2 7AY, UK

⁵Department de Física, Faculdade de Ciências, Universidade do Porto,
Rua do Campo Alegre 687, 4169-007 Porto, Portugal.

⁶Department of Physics and Optical Science, University of North Carolina at Charlotte,
Charlotte, North Carolina 28223, USA

*Corresponding author: h-aref@cc.sbu.ac.ir

Received 24 November 2009; revised 3 February 2010; accepted 2 March 2010;
posted 11 March 2010 (Doc. ID 120469); published 29 March 2010

We study the measurand-induced spectral shift of the photonic bandgap edge of a hollow-core photonic crystal fiber. The physical measurands considered are strain, temperature, curvature, and twist. A noticeable sensitivity to strain, temperature, and twist is observed, with a blueshift to increase strain and twist. An increase in temperature induces a redshift. On the other hand, curvature has no observable effect on the spectral position of the photonic bandgap edge. © 2010 Optical Society of America

OCIS codes: 060.4005, 060.2370, 060.5295.

1. Introduction

The guidance property of hollow core (HC) photonic crystal fibers (PCFs) is dictated by a periodic structure layout in the fiber cladding that induces a photonic bandgap (PBG) behavior. The cladding of the fiber acts as a periodic crystal that forbids propagation of light in specific wavelength ranges. Light with wavelengths in these bandgaps can be confined inside the air core and propagates along it [1]. The air core of these fibers is formed by removing a certain number of central capillaries from the stacked preform.

The development of sensors based on HC PCF is a recent and active research topic in the context of fiber optic sensing. Particularly relevant is the application of these fibers for gas sensing in the face of the large overlap of the optical field with the measurement volume [2,3], but other measurands have also been considered, for example, curvature [4] and strain and temperature [5] as well as humidity [6]. Recently, an acoustic hydrostatic pressure sensor based on HC PCF was reported and the sensitivity of the sensor has been compared with others based on conventional single-mode fibers (SMFs) [7]. In general, the potential of these fibers for sensing is substantial, and it would certainly be strengthened with new approaches to detect the measurand interaction with the fiber.

The PBG property of HC PCF is a function of the refractive-index contrast in the fiber cross section as well as of its geometry. Studying the PBG shift when the refractive-index contrast changes has been done using the scaling law technique [8,9]. This strategy is similar to the well-known and widely used scaling laws that describe the shift in the bandgap when the size scale of the fiber is altered [10], following the well-known length scale law discussed in depth by Joannopoulos *et al.* [11]. Using the scalar-wave approximation, simple index scaling laws have been derived [9] that predict the way the photonic states of the fiber scale with changes in the refractive-index contrast. Furthermore, scaling laws can be useful in other fields of fiber technology [10]. Recently, there has been increased interest in bandgap fibers made from materials other than silica and air, which are the materials of most common HC PCFs. For example, high-index glasses can be used for guidance in the infrared region of the spectrum [12], whereas tunable fiber devices can be made by filling the holes of a photonic crystal fiber with liquid crystals [13,14]. All these applications require fibers of different index contrasts between the high and the low refractive-index regions of the photonic crystal cladding of the fiber. We have characterized the spectral shift of the PBG edge of a HC PCF induced by physical measurands such as strain, temperature, curvature, and twist.

2. Principle of Operation

To characterize the measurand-induced spectral shift of the PBG edge, a piece of HC PCF was spliced directly between two lengths of SMF. For this purpose we considered a bandgap fiber that was designed and fabricated at the University of Bath.. The bandgap of this fiber, shown in Fig. 1(a), is a seven-cell HC PCF with a core diameter of $\sim 15 \mu\text{m}$ and an outside diam-

eter of $\sim 125 \mu\text{m}$ [Fig. 1(b)], with a PBG edge at shorter wavelengths around 1540 nm.

It has been observed that the loss pattern of PBG fibers in the PBG edge region is a function of the fiber length, particularly when small lengths are considered, i.e., after light propagation along 100–200 m of PCF the spectral features of the bandgap essentially stabilize. This process involves the shift of the low-wavelength edge to longer wavelengths (together with the disappearance of spectral transmission oscillations located to the left of the bandgap), and the shift of the high-wavelength edge to lower wavelengths [15]. Therefore, we observed a bandgap spectrum narrowing with a longer fiber length. Studies indicate that this effect in the bandgap low-wavelength region is dominated by the loss via coupling to fiber surface modes [16]. The mechanism by which light is leaked out can be either by intrinsic loss of the surface mode or by coupling of the latter to a continuum of leaky modes. On the long-wavelength side of the bandgap, the shift of the edge is owed to the fact that the fundamental mode is no longer supported and higher-order modes propagate, which show higher losses and therefore disappear after some propagation length, which permits the appearance of an effective bandgap edge.

Focusing on the wavelength region close to the low-wavelength edge of the bandgap, coupling to fiber surface modes in practical HC PCF is promoted by tunneling mechanisms [17]. The light in this region is less well confined and, therefore, it is natural to deduce that the action on fiber of some physical parameters should accompany a relatively strong loss in fiber. The motivation for our research was to verify this hypothesis and to quantify the effect of physical measurands on fiber. Indeed, some previous results already pointed out this path [8–10]. As indicated above, the description of a PBG edge shift that is due to changes in the refractive-index contrast of

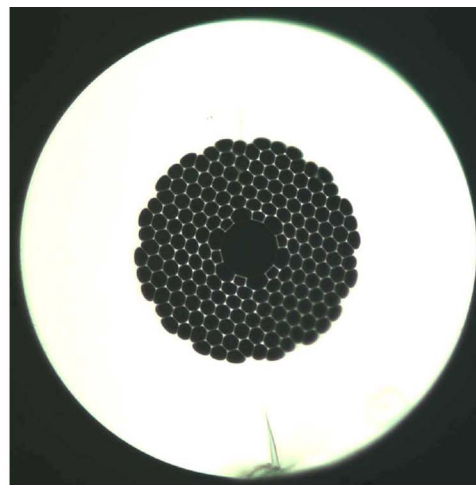
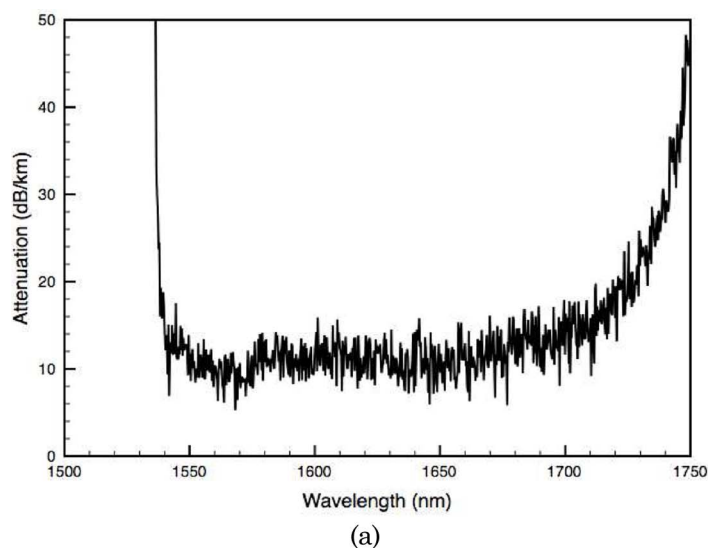


Fig. 1. (Color online) (a) Transmission spectrum of the bandgap fiber considered for characterization of measurand-induced effects on the PBG edge and (b) optical microscope image of the cross section of the selected fiber.

HC PCF is simply evaluated by using the refractive-index scaling law, which is based on the scalar waveguide approximation [9,10]. Based on these findings, Antonopoulos and co-workers reported an experimental demonstration of the frequency shift of the PBG edge that is due to refractive-index scaling using D₂O-filled HC PCFs [10]. Also, Sun and Chan [8] reported the use of PBG fibers as a refractive-index sensor and described its behavior based again on refractive-index scaling laws. In general, it can be expected that some physical measurands can change the PBG property of HC PCF due to changes in refractive-index contrast and geometric effects, therefore inducing a PBG spectral shift.

3. Experimental Setup

The experimental setup is shown in Fig. 2. The light source used was an Er-doped fiber with amplified spontaneous emission, central wavelength, and full width at half-maximum of 1.8 mW, 1550 nm, and 60 nm, respectively. The output transmission spectrum was observed with an optical spectrum analyzer (OSA). By means of a conventional fusion splicer (Fujikura SM40), the HC PCF was spliced at both ends to SMFs. All the splicing was done manually, and the optimum parameters were obtained after some attempts to achieve minimum fusion loss. This resulted in 0 bit (bit is Fujikura's internal unit that is used for arc current) and 400 ms for the power and arc time duration, respectively, and a typical splice loss of 1.5 dB. The length of the HC fiber was ~28 cm.

To investigate the strain effect on the spectral position of the bandgap edge, two micropositioners were used to fix the SMF fibers and to apply strain. With regard to the effect of temperature, the HC PCF was placed inside a vessel of heated water and the measurements were taken during the cooling period.

To apply torsion to the HC PCF, one of the holding stages could be rotated while the other was stationary. By moving longitudinally one holder relative to the other, curvature could also be applied to the HC PCF.

4. Results and Discussion

When strain is applied to the HC PCF, we observed a spectral shift of the PBG, as indicated in Fig. 3, which shows the shift of the PBG edge [Fig. 3(a)], the variation of the transmission in one wavelength in the edge located approximately at the middle of the edge [Fig. 3(b)], and the transmission at a wavelength located in the PBG passband [Fig. 3(c)]. These results indicate a blueshift of the PBG edge with the increase of strain (slope of approximately $-0.7 \text{ pm}/\mu\epsilon$). For wavelengths located approximately in the middle of the edge, Fig. 3(b) shows that the loss dependence on a logarithmic scale with strain associated with the PBG edge shift is fairly linear, with a slope of $-0.0018 \text{ dB}/\mu\epsilon$. As expected, within the passband of the bandgap, the transmission is independent of applied strain.

Figure 4 shows the results relative to variations of temperature [Fig. 4(a), edge shift; Fig. 4(b), transmission at approximately the middle of the edge]. Different from what happens in the case of strain, now a temperature increase results in a redshift of the PBG edge with a slope of $\sim 29 \text{ nm}/^\circ\text{C}$. The results obtained when curvature was applied to the HC PCF are shown in Fig. 5. It is clear that this parameter does not affect the PBG. Figure 6 shows data relative to the application of twist to the HC PCF. A redshift was observed at the PBG edge that was fairly symmetric considering the clockwise or counterclockwise twist orientations.

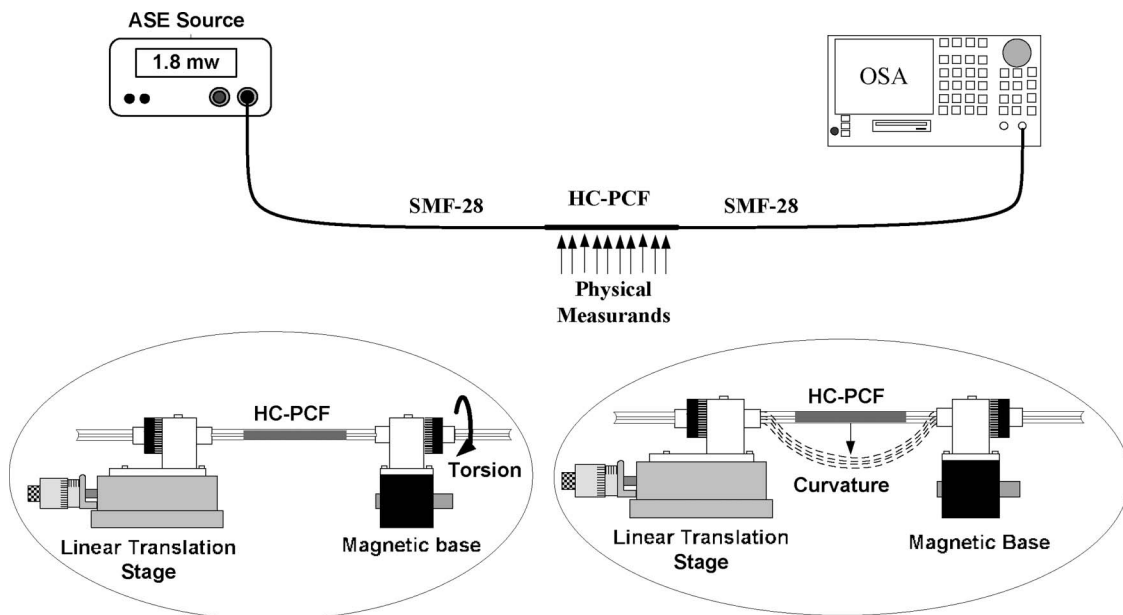


Fig. 2. Experimental setup for the characterization of the measurand-induced shift of the edge of the spectral bandgap; also shown is the configuration that was used to apply torsion and curvature to the HC PCF.

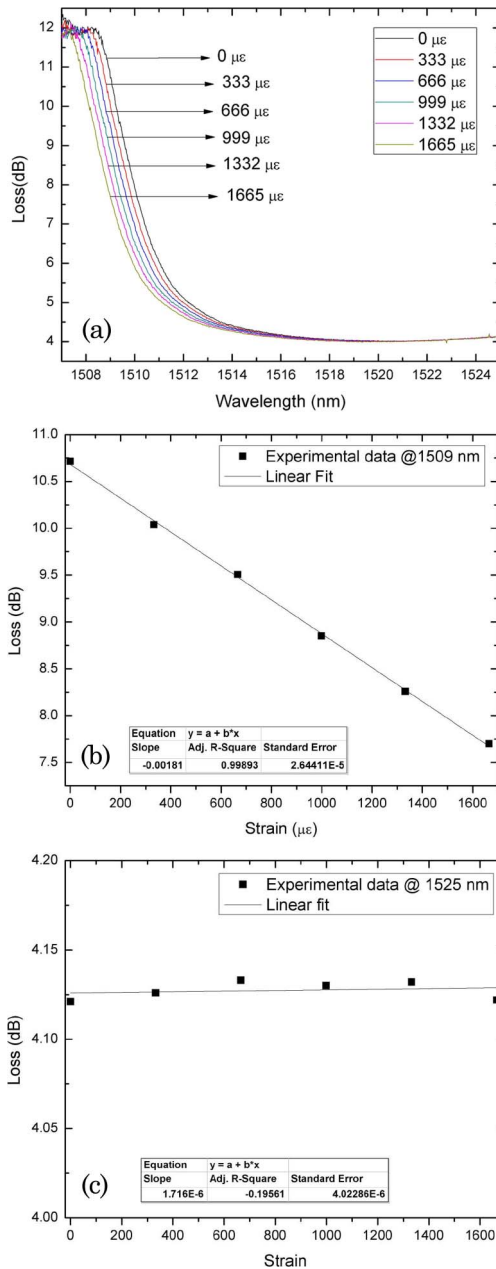


Fig. 3. (Color online) Effect of applied strain to the HC PCF on (a) the spectral position of the PBG lower wavelength edge, (b) the loss variation at wavelength 1509 nm located in the PBG edge, (c) the loss variation at wavelength 1525 nm located in the PBG passband region.

The PBG process is a complex phenomenon, and the interpretation of the changes induced in the fiber transmission by strain, temperature, and twist requires a theoretical study of the problem and its computational simulation. However, the results obtained indicate that the measurand-induced shift of the PBG edge of hollow-core fibers can be used as the basis for sensing configurations supported by this type of fiber. Figure 1(a) shows that the edge slope can be large, which is favorable for high sensitivity readout. Compensation for optical power fluctuations can be obtained if we take into consideration

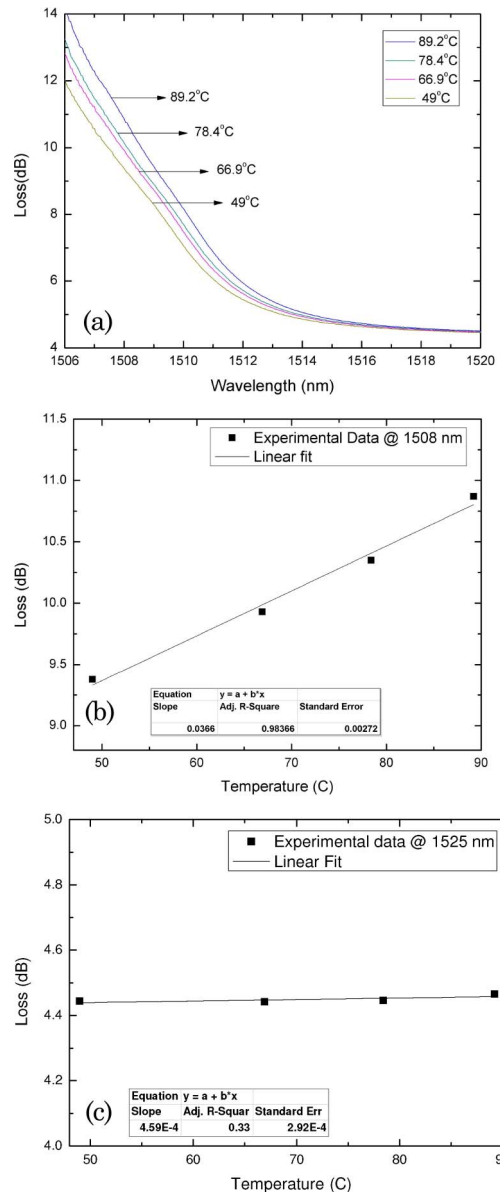


Fig. 4. (Color online) Effect of temperature variation on (a) the spectral position of the PBG lower wavelength edge, (b) the loss variation at wavelength 1508 nm located in the PBG edge, (c) the transmission versus temperature at wavelength 1525 nm located in the PBG passband region.

a second wavelength in the PBG passband where its transmission is essentially independent of the measurand value.

We have presented results that show it is feasible to apply HC PCFs as sensing elements based on the measurand-induced PBG edge shift. But it is also feasible to apply these fibers for optical demodulation of signals coming from other sensing heads, where the tunability of the PBG edge provides additional flexibility. An example of this role is within the context of fiber Bragg grating (FBG) interrogation [18,19]. Indeed, when dealing with FBG sensors, the conversion of the measurand-induced wavelength modulation into an optical intensity modulation can be performed

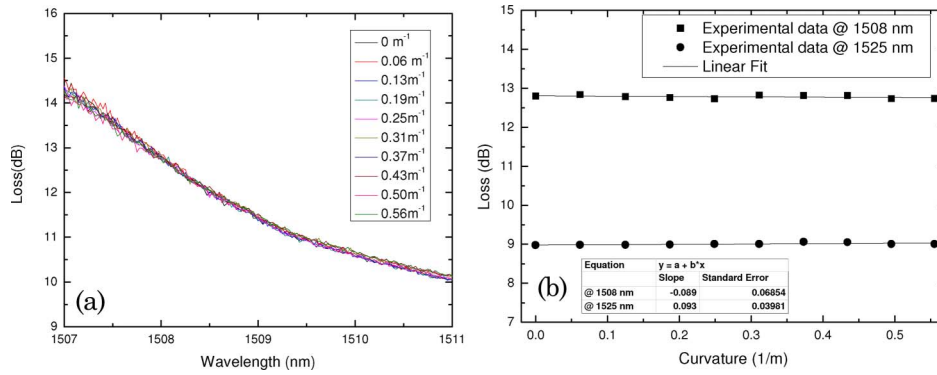


Fig. 5. (Color online) (a) PBG edge shift due to curvature variation and (b) transmission versus curvature at wavelengths of 1508 nm (located in the PBG edge region) and 1525 nm (located in the PBG passband region).

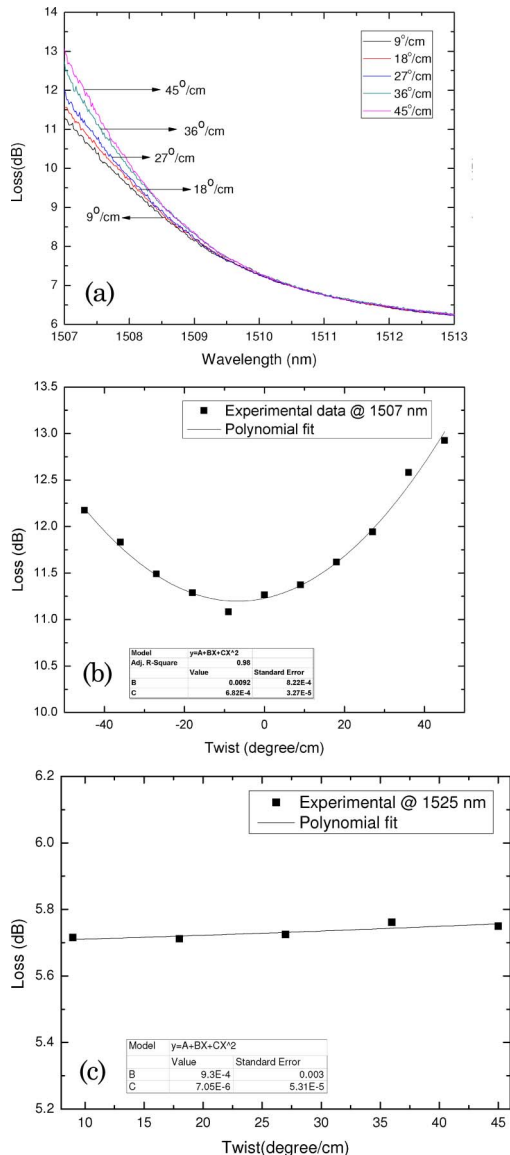


Fig. 6. (Color online) Effect of twist applied to the HC PCF on (a) the spectral position of the PBG lower wavelength edge, (b) the loss variation at wavelength 1507 nm located in the PBG edge, (c) the transmission versus twist at wavelength 1525 nm located in the PBG passband region.

when the light that returns from the FBG propagates through a length of HC PCF located in the control region, with the tuning of the PBG edge to the optimum sensitivity position achieved by application of strain to this fiber. Certainly, many other possibilities can be thought of, but the most relevant factor to point out is the dual functionality of HC PCF, i.e., the freedom to use this type of fiber as a sensing or a processing element. This characteristic can be advantageous in several fiber optic sensing applications, and a systematic study of its potential is currently under way.

5. Conclusion

We have presented the measurand-induced spectral shift of the photonic bandgap edge of a hollow-core photonic crystal fiber. The physical measurands considered were strain, temperature, curvature, and twist. To increase strain a blueshift was observed in the spectral position of the PBG edge, whereas a redshift appears for temperature and twist. Curvature does not introduce a noticeable change in the bandgap edge. These characteristics indicate the feasibility of using this type of fiber for sensing as well as for optical signal processing.

The authors acknowledge the research and development environment provided by the Framework Programme (FP6) Project, NextGenPCF of the European Union, IST 34918: Next Generation Photonic Crystal Fibers.

References

1. R. F. Cregan, B. J. Mangan, J. C. Knight, T. A. Birks, P. St. J. Russell, P. J. Roberts, and D. C. Allan, "Single-mode photonic band gap guidance of light in air," *Science* **285**, 1537–1539 (1999).
2. R. Thapa, K. Knabe, K. L. Corwin, and B. R. Washburn, "Arc fusion splicing of hollow-core photonic bandgap fibers for gas-filled fiber cells," *Opt. Express* **14**, 9576–9583 (2006).
3. Y. L. Hoo, W. Jin, H. L. Ho, J. Ju, and D. N. Wang, "Gas diffusion measurement using hollow-core photonic bandgap fiber," *Sens. Actuators B* **105**, 183–186 (2005).
4. W. N. MacPherson, M. J. Gander, R. McBride, J. D. C. Jones, P. M. Blanchard, J. G. Burnett, A. H. Greenaway, B. Mangan, T. A. Birks, J. C. Knight, and P. St. J. Russell, "Remotely addressed optical fiber curvature sensor using multicore photonic crystal fiber," *Opt. Commun.* **193**, 97–104 (2001).

5. S. H. Aref, R. Amezcua-Correa, J. P. Carvalho, O. Frazão, P. Caldas, J. L. Santos, F. M. Araújo, H. Latifi, F. Farahi, L. A. Ferreira, and J. C. Knight, "Modal interferometer based on hollow-core photonic crystal fiber for strain and temperature measurement," *Opt. Express* **17**, 18669–18675 (2009).
6. I. Hidalgo, R. Goya, I. R. Matías, F. J. Arregui, and R. O. Claus, "Humidity evanescent hollow core fiber sensor," *Proc. IEEE* **3**, 1214–1217 (2004).
7. M. Pang and W. Jin, "Detection of acoustic pressure with hollow-core photonic bandgap fiber," *Opt. Express* **17**, 11088–11097 (2009).
8. J. Sun and C. Chan, "Photonic bandgap fiber for refractive index measurement," *Sens. Actuators B* **128**, 46–50 (2007).
9. T. A. Birks, D. M. Bird, T. D. Hedley, J. M. Pottage, and P. St. J. Russell, "Scaling laws and vector effects in bandgap-guiding fibers," *Opt. Express* **12**, 69–74 (2004).
10. G. Antonopoulos, F. Benabid, T. A. Birks, D. M. Bird, J. C. Knight, and P. St. J. Russell, "Experimental demonstration of the frequency shift of bandgaps in photonic crystal fibers due to refractive index scaling," *Opt. Express* **14**, 3000–3006 (2006).
11. J. D. Joannopoulos, R. D. Meade, and J. N. Winn, *Photonic Crystals* (Princeton U. Press, 1995), pp. 19–20.
12. G. J. Pearce, J. M. Pottage, D. M. Bird, P. J. Roberts, J. C. Knight, and P. St. J. Russell, "Hollow-core PCF for guidance in the mid to far infra-red," *Opt. Express* **13**, 6937–6946 (2005).
13. R. T. Bise, R. S. Windeler, K. S. Kranz, C. Kerbage, B. J. Eggleton, and D. J. Trevor, "Tunable photonic bandgap fiber," in *Optical Fiber Communication Conference*, Vol. 70 of OSA Trends in Optics and Photonic (Optical Society of America, 2002), pp. 466–468.
14. T. R. Wolinski, A. Czaplá, S. Ertman, M. Tefelska, A. W. Domanski, J. Wójcik, E. Nowinowski-Kruszelnicki, and R. Dabrowski, "Photonic liquid crystal fibers for sensing applications," *IEEE Trans. Instrum. Meas.* **57**, 1796–1802 (2008).
15. F. Benabid, "Hollow-core photonic bandgap fibre: New light guidance for new science and technology," *Philos. Trans. R. Soc. London Ser. A* **364**, 3439–3462 (2006).
16. J. A. West, C. M. Smith, N. F. Borrelli, D. C. Allan, and K. W. Koch, "Surface modes in aircore photonic band-gap fibers," *Opt. Express* **12**, 1485–1495 (2004).
17. F. Couny, H. Sabert, P. J. Roberts, D. P. Williams, A. Tomlinson, B. J. Mangan, L. Farr, J. C. Knight, T. A. Birks, and P. St. J. Russell, "Visualizing the photonic band gap in hollow core photonic crystal fibers," *Opt. Express* **13**, 558–563 (2005).
18. J. M. López-Higuera, ed., *Handbook of Optical Fiber Sensing Technology* (Wiley, 2002), Chap. 18.
19. L. A. Ferreira, J. L. Santos, E. V. Diatzikis, and F. Farahi, "Frequency modulated multimode laser diode for fiber Bragg grating sensors," *J. Lightwave Technol.* **16**, 1620–1630 (1998).